



OPEN ACCESS

EDITED BY

Claudia U. Duerr,
CharitéUniversity Medicine Berlin,
Germany

REVIEWED BY

Martijn J. Schuijs,
Flemish Institute for Biotechnology, Belgium
Irene Mattiola,
CharitéUniversity Medicine Berlin,
Germany

*CORRESPONDENCE

Laurent Derré
✉ laurent.derre@chuv.ch

RECEIVED 08 November 2023

ACCEPTED 20 December 2023

PUBLISHED 12 January 2024

CITATION

Schneider AK, Domingos-Pereira S, Cesson V,
Polak L, Fallon PG, Zhu J, Roth B, Nardelli-
Haefliger D and Derré L (2024) Type 2
innate lymphoid cells are not involved in
mouse bladder tumor development.
Front. Immunol. 14:1335326.
doi: 10.3389/fimmu.2023.1335326

COPYRIGHT

© 2024 Schneider, Domingos-Pereira, Cesson,
Polak, Fallon, Zhu, Roth, Nardelli-Haefliger and
Derré. This is an open-access article distributed
under the terms of the [Creative Commons
Attribution License \(CC BY\)](#). The use,
distribution or reproduction in other forums
is permitted, provided the original author(s)
and the copyright owner(s) are credited and
that the original publication in this journal is
cited, in accordance with accepted academic
practice. No use, distribution or reproduction
is permitted which does not comply with
these terms.

Type 2 innate lymphoid cells are not involved in mouse bladder tumor development

Anna K. Schneider¹, Sonia Domingos-Pereira¹, Valérie Cesson¹,
Lenka Polak¹, Padraic G. Fallon², Jinfang Zhu³, Beat Roth¹,
Denise Nardelli-Haefliger¹ and Laurent Derré^{1*}

¹Urology Research Unit and Urology Biobank, Department of Urology, Centre Hospitalier Universitaire Vaudois, Lausanne, Switzerland, ²School of Medicine, Trinity Biomedical Sciences Institute, Trinity College Dublin, Dublin, Ireland, ³Molecular and Cellular Immunoregulation Section, Laboratory of Immune System Biology, National Institute of Allergy and Infectious Diseases, National Institutes of Health, Bethesda, MD, United States

Therapies for bladder cancer patients are limited by side effects and failures, highlighting the need for novel targets to improve disease management. Given the emerging evidence highlighting the key role of innate lymphoid cell subsets, especially type 2 innate lymphoid cells (ILC2s), in shaping the tumor microenvironment and immune responses, we investigated the contribution of ILC2s in bladder tumor development. Using the orthotopic murine MB49 bladder tumor model, we found a strong enrichment of ILC2s in the bladder under steady-state conditions, comparable to that in the lung. However, as tumors grew, we observed an increase in ILC1s but no changes in ILC2s. Targeting ILC2s by blocking IL-4/IL-13 signaling pathways, IL-5, or IL-33 receptor, or using IL-33-deficient or ILC2-deficient mice, did not affect mice survival following bladder tumor implantation. Overall, these results suggest that ILC2s do not contribute significantly to bladder tumor development, yet further investigations are required to confirm these results in bladder cancer patients.

KEYWORDS

innate lymphoid cell (ILC), type 2 innate lymphoid cell (ILC2), bladder cancer, tumor microenvironment, MB49 bladder tumor model

Introduction

Bladder cancer ranks as the 10th most common cancer worldwide (1). The risk of developing a bladder cancer increases with age, smoking, and exposition to certain chemicals (1–3). Urothelial carcinoma represents 90% of bladder cancer cases and can be classified into two main subtypes: non-muscle invasive bladder cancer (NMIBC), confined to the urothelium or lamina propria, and muscle-invasive bladder cancer (MIBC), characterized by invasion into the detrusor muscle or adjacent tissues, with potential metastasis (4, 5). The gold-standard treatments for NMIBC and MIBC are

intravesical Bacillus Calmette Guérin (BCG) instillations and cystectomy with or without chemotherapy, respectively. These treatments are limited by significant side effects and failure highlighting the need to investigate novel therapeutic targets to improve the disease management (6).

Identified a decade ago, innate lymphoid cells (ILCs) are viewed as the innate counterpart of CD4 T helper (T_H) cells (7). They are lymphocytes lacking antigen receptor and classical phenotypic markers for lymphoid and myeloid cells yet exhibit similar functions as T_H cells (7, 8). Among the different ILC subsets (9), type 2 innate lymphoid cells (ILC2) are considered as the innate counterpart of T_H2 cells, and are characterized by their ability to produce type 2 cytokines including IL-4, IL-5 and IL-13 (7, 8). They express the transcription factors GATA-binding protein 3 (Gata3) and retinoic acid receptor-related orphan receptor alpha ($ROR\alpha$), which play crucial roles in their development and function (10–12). ILC2s are generally tissue-resident cells particularly enriched in mucosal and barrier tissues such as the skin, intestine, and lung (8, 13), and rapidly respond to environment changes by sensing factors including neuropeptides, cytokines and alarmins such as IL-25, IL-33 and thymic stromal lymphopoietin released by epithelial and/or myeloid cells under infection or tissue damage (14, 15). While ILC2s are crucial for host defense and tissue homeostasis, their dysregulation has been implicated in inflammatory diseases and allergic responses, including asthma where ILC2s promote airway inflammation leading to airway hyperresponsiveness (16, 17).

Emerging evidence suggests that ILCs, including ILC2s, play significant roles in shaping the tumor microenvironment and anti-tumor immune response (18–21). Tumor-infiltrating ILC2s have been reported to exert anti-tumor activity through direct interaction with T cells (22) or by inducing the recruitment of innate immune cells to the tumor such as eosinophils and dendritic cells, thereby improving T cell-mediated anti-tumor response in melanoma and pancreatic ductal adenocarcinoma (23, 24). However, the presence of ILC2s within the tumor has also been associated with a diminished anti-tumor response (25). Notably, ILC2s have been reported to exert pro-tumoral role by limiting the anti-tumor functions of natural killer cells, promoting tumor burden (26). In addition, ILC2-expressed chemokines and cytokines, particularly CXCL2 and IL-13, have been implicated in the recruitment of immunosuppressive cells such as neutrophils or myeloid-derived suppressor cells (MDSC) into the tumor microenvironment, as observed in hepatocellular carcinoma, breast cancer, and colorectal cancer (27–29). In bladder cancer, our group recently showed that ILC2s detected in the urine of NMIBC patients undergoing BCG treatment, were positively correlated with the frequency of urinary MDSCs and linked to bladder tumor recurrence (30), suggesting a key role of ILC2s in bladder cancer. Overall, the role of ILC2s in cancer is still under debate and seems to depend on the studied model and the type of tumor. Thus, better understanding of their contribution in bladder tumor development is needed before harnessing them for immunotherapy.

In this study, we investigated the involvement of ILC2s in bladder tumor using mouse models. We found the mouse bladder

as being particularly enriched in ILC2s at steady state, but their number did not change upon tumor growth. In addition, targeting ILC2s using neutralizing antibodies or different transgenic mouse models did not impact mice survival following bladder tumor challenge. Overall, these data suggest that ILC2s do not contribute significantly to bladder tumor development.

Results

High frequency of ILC2s in the murine bladder

To assess the presence of ILCs in the bladder, we conducted a comparative analysis of ILC infiltration in different organs at steady state (i.e., without tumor). Flow cytometry analysis was performed to evaluate the infiltration of total ILCs, ILC1s, ILC2s and ILC3s (Figure 1A, Supplementary Figure 1A) in the bladder, the spleen and iliac lymph nodes (bladder draining lymph nodes; ILN). As control, we also included the lung, and lamina propria of the small intestine (LP-SI), two well-known homing sites for ILC2s and ILC3s, respectively (Supplementary Figure 1A) (13, 16). Interestingly, the frequency of ILCs among CD45⁺ cells in the bladder was comparable to that observed in the LP-SI, and significantly higher than in the lung, spleen, and ILN (Figure 1B). However, due to a limited infiltration of total immune cells into the bladder at steady state (Supplementary Figure 1B), the absolute number of total ILCs infiltrating the bladder was significantly lower compared to the other organs (Figure 1C). Among bladder ILC subsets, we surprisingly found a very high frequency of ILC2s (ca. 70% of total ILCs), comparable to that in the lung (Figure 1D). In addition, while the frequency of ILC3s was barely detectable, the proportion of ILC1s was higher in the bladder compared to both the lung and lamina propria. Overall, ILC2s represented the predominant ILC subset in the bladder (Supplementary Figure 1C). However, the absolute number of ILC subsets infiltrating the bladder was significantly lower compared to the lung and LP-SI (Figure 1E).

Bladder-infiltrating ILC2s remained stable upon tumor growth, while ILC1 absolute number increased

To investigate the potential role of ILC2s in bladder tumor development, we next characterized the changes in bladder ILC infiltration throughout tumor growth, using the orthotopic murine MB49 bladder tumor model. Luciferase-expressing MB49 tumor cells were used to monitor tumor establishment and growth via *in vivo* bioluminescent imaging. Bladder cells obtained from mice at different time points after bladder tumor implantation (day 5, 10 and 14) were analyzed for ILC subsets and compared to bladder cells recovered from mice without tumor (Figure 2A). Of note, due to a high variability in bladder weight during tumor growth

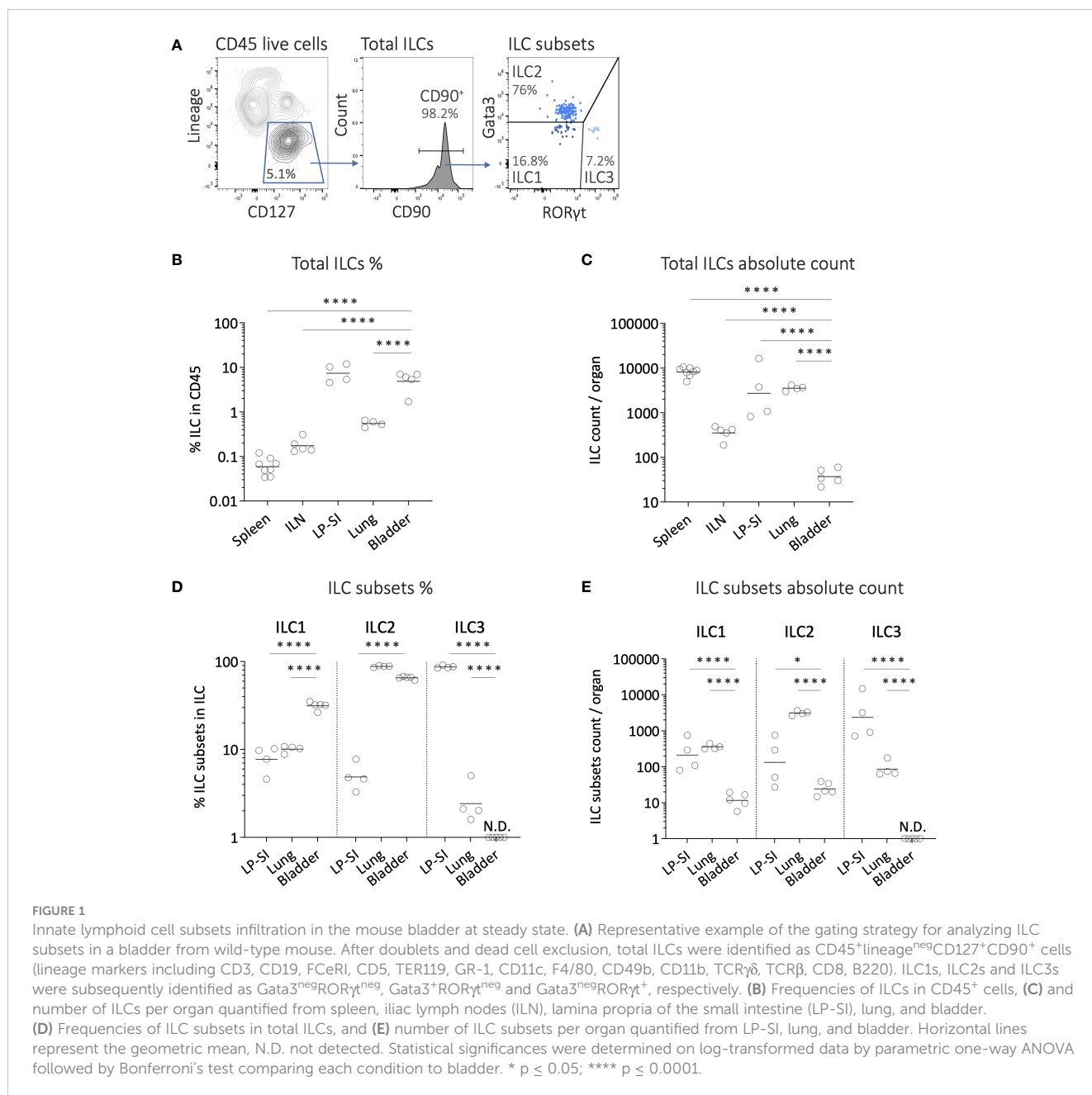
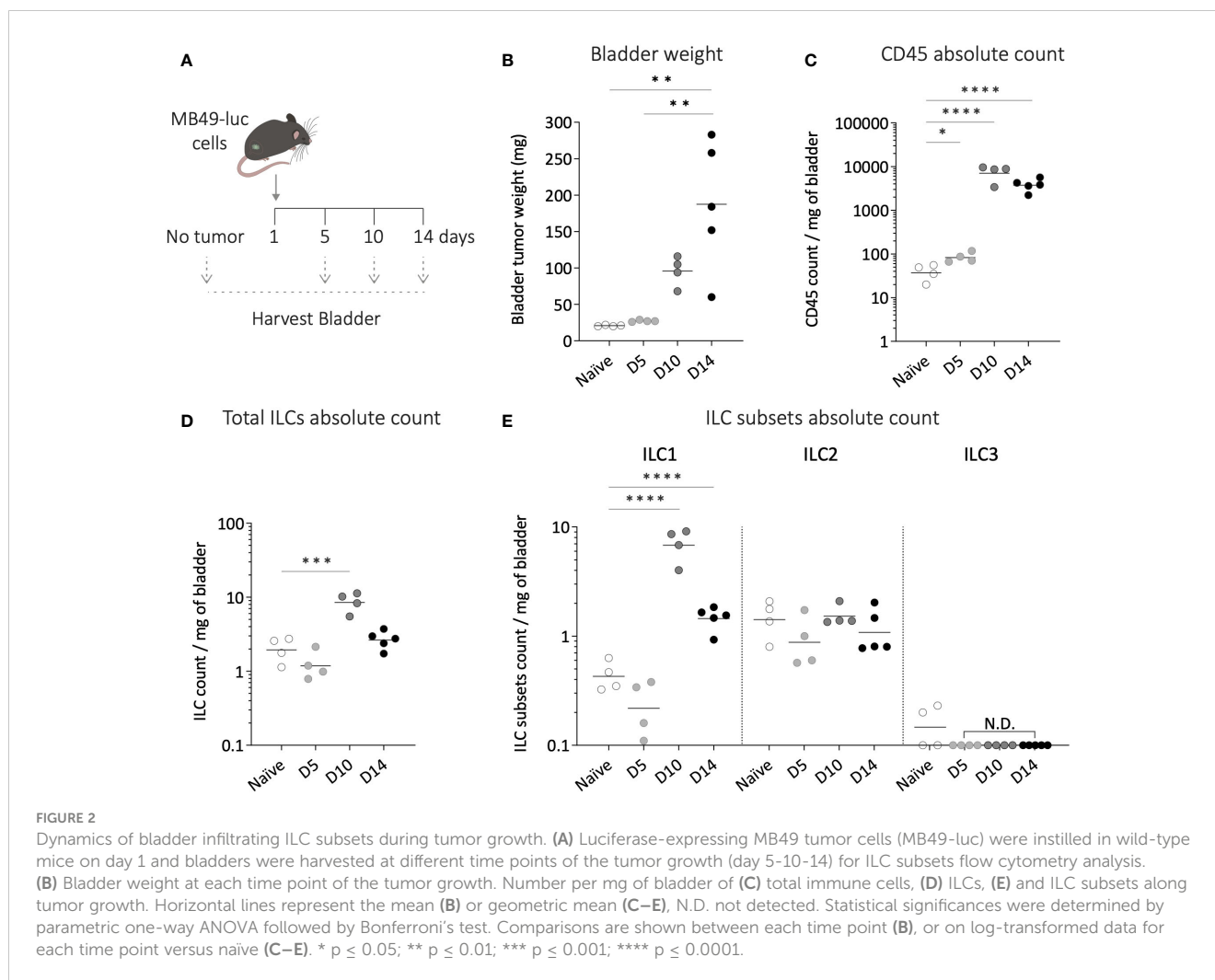


(Figure 2B), immune cell absolute numbers were normalized to the bladder weight at each time point. We observed a significant increase in the absolute number of total immune cells infiltrating the bladder during tumor growth (Figure 2C). ILC infiltration displayed a significant increase only on day 10 of tumor development (Figure 2D). Compared to the fold-increase in the total population of immune cells, ILCs did not represent the main subset expanding significantly with tumor growth.

Among the different ILC subsets, the bladder exhibited comparable infiltration levels during steady state and early tumor growth (D5), with ILC2s remaining the most abundant subset (Figure 2E). However, as the tumor grew, the number of ILC1s

per milligram of bladder significantly increased, reaching a ca. 10-fold increase on day 10, this subpopulation becoming the predominant ILC subset in the bladder. In contrast, the level of ILC2s remained stable throughout tumor growth, while ILC3s remained almost undetectable (Figure 2E).

We also evaluated the functional status of ILC2s from the bladder by assessing their capacity to secrete IL-13 (20). Upon *in vitro* stimulation, ILC2s from both bladder tumor-free and tumor-bearing mice secreted IL-13, with a significant increase in secretion levels observed in the presence of the tumor (Supplementary Figure 2). These results suggest that bladder-infiltrating ILC2s are functional, even in the presence of bladder tumor.



Inhibiting ILC2 activation and function did not alter mice survival after bladder-tumor challenge

To investigate whether ILC2s may alter the bladder tumor development, we studied the effects of targeting ILC2 pathways on tumor growth and mice survival. We first quantified the concentrations of cytokines known to be involved in ILC2s activation and function (20) by luminex assay in bladder samples from tumor-free mice (naïve) and during tumor growth (day 5, 10, and 13) (Figure 3A). At steady state, IL-13 and IL-33 were present in the bladder, while IL-4 was undetectable, and IL-5 and IL-25 levels were close to the detection limit. During tumor growth, although IL-13 levels substantially dropped to a very low level, and IL-25 remained very low, IL-4, IL-5, and IL-33 levels significantly increased, with a peak observed only on day 10 for IL-5, suggesting that IL-4, IL-5, and IL-33 related pathways may be activated along bladder tumor growth. Thus, to inhibit ILC2 functions, mice were treated with a blocking antibody targeting IL-4R α (CD124) (31–33). No differences compared to the control mice were observed in tumor growth (Supplementary Figure 3A), or in mouse survival (Figure 3B). Then we inhibited ILC2 functions by

targeting IL-5 using a blocking antibody (34). Similar to the blocking of IL-4R α , no differences in tumor growth (Supplementary Figure 3B) or mouse survival (Figure 3C) were observed when compared to the control mice.

We next inhibited ILC2 activation by targeting IL-33R α (ST2). IL-33 signaling through its receptor ST2 has been reported as a key pathway for inducing the secretion of type 2 cytokines by ILC2s, and neutralizing ST2 *in vivo* significantly limited ILC2 activation (35–37). We first confirmed the high expression of ST2 by bladder ILC2s compared to ILC1s and 3, which remained stable along the bladder tumor growth (Supplementary Figure 3C), consistent with previous observations (38) and suggesting that bladder ILC2s may be responsive to IL-33. Mice were then treated with an anti-ST2 blocking antibody (Figure 3D). No significant differences in tumor growth were observed compared to the control mice (Supplementary Figure 3D), and no changes in survival were detected (Figure 3D). Similar results were obtained when using IL-33-deficient mice (Supplementary Figure 3E, Figure 3E), which are known to exhibit reduced ILC2 infiltration in tissues and/or less functionally competent ILC2s (39–41). Overall, these data suggest that ILC2 may not play a critical role in bladder tumor development.

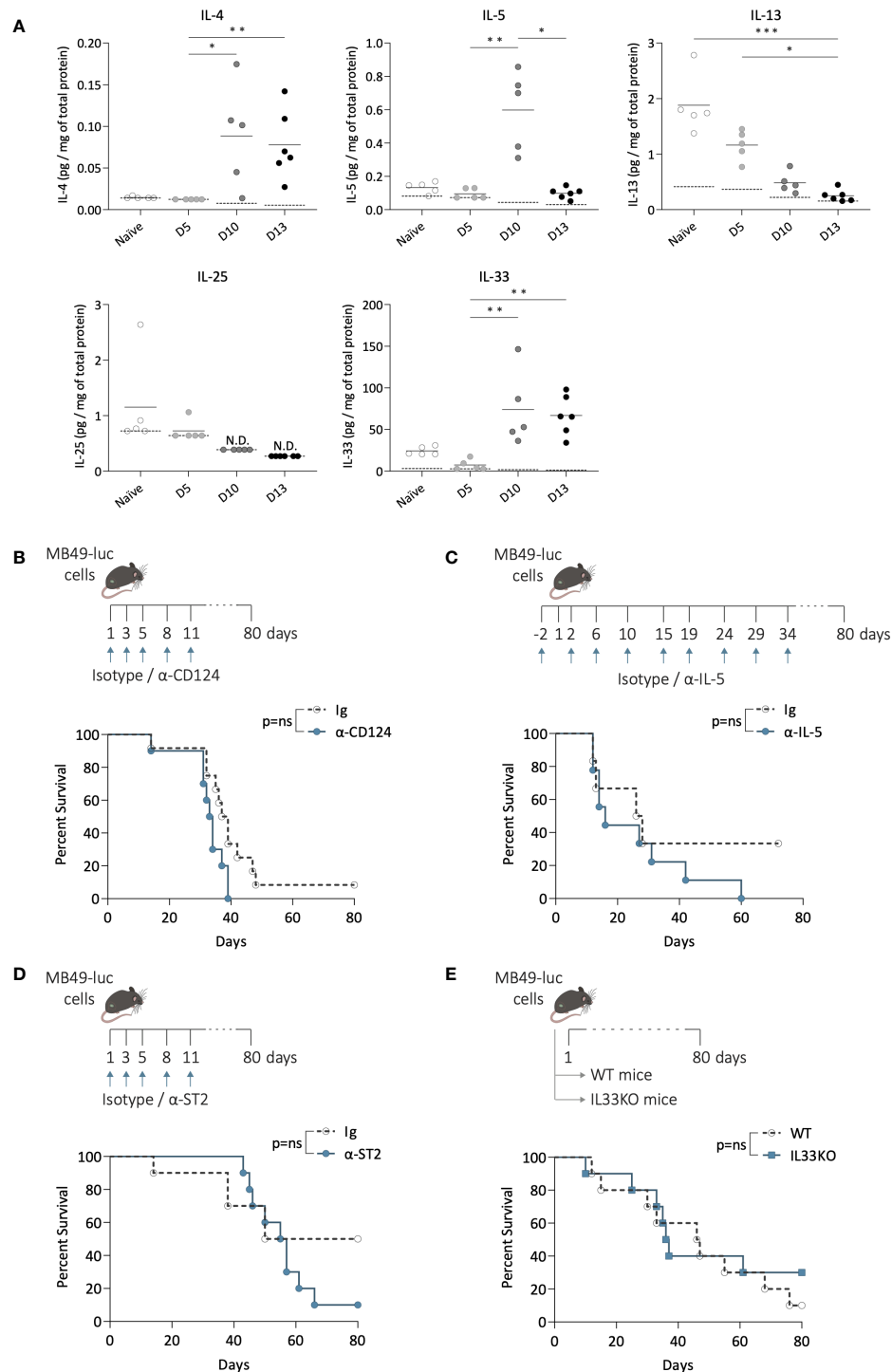


FIGURE 3

Inhibition of ILC2 activation and function during bladder tumor challenge. **(A)** Level of IL-4, IL-5, IL-13, IL-25 and IL-33 per mg of total protein in bladders of mice without tumors (naïve) and at indicated time point after tumor instillation (day 5, 10, and 13). Horizontal solid lines represent the mean, and the dotted lines represent the limit of detection, N.D. not detected. Statistical significances were determined by one-way ANOVA followed by Dunn's test comparing the different time points for each cytokine. **(B–D)** Mice were treated i.p. with blocking antibodies or isotypes control at indicated days (arrows) and instilled with MB49 tumor cells in the bladder at day 1. **(B)** Survival curves of mice treated with α-CD124 (n=10) or isotype control (Ig; n=12), or **(C)** with α-IL-5 (n=9) or isotype control (Ig; n=6), or **(D)** with α-ST2 (n=10) or isotype control (Ig; n=10). **(E)** Survival curves of wild-type (WT; n=10) and IL-33-deficient (IL33KO; n=10) mice after bladder tumor implantation. Log-rank test was performed as statistical analysis for survival curves. * $p \leq 0.05$; ** $p \leq 0.01$; *** $p \leq 0.001$; ns: not significant.

Depletion of ILC2s did not impact mice survival after bladder-tumor challenge

We finally studied bladder tumor development in mice lacking ILC2s, using $Ror\alpha^{Cre}Gata3^{fl/fl}$ ILC2-deficient mice (42). We first evaluated the extent of ILC2 deficiency in these mice compared to their littermate controls ($Gata3^{fl/fl}$) under steady-state conditions (Figure 4A). Flow cytometry analysis revealed a significant reduction in the number of ILCs in the bladders of $Ror\alpha^{Cre}Gata3^{fl/fl}$ mice compared to the littermate controls (Figure 4B). Among the different ILC subsets, ILC2s were nearly undetectable in the bladders of ILC2-deficient mice, while the infiltration of ILC1s and ILC3s remained unchanged compared to the littermate controls (Figure 4C). In addition, there were no differences in the T-cell compartment, CD11b, and NK cells between ILC2-deficient mice and littermate controls (Supplementary Figure 4A). These data confirmed the specific depletion of ILC2s in $Ror\alpha^{Cre}Gata3^{fl/fl}$ mice. Then tumor was implanted in the bladder of ILC2-deficient mice and littermates (Figure 4D). The absence of ILC2s did not affect bladder tumor development (Supplementary Figure 4B) or the mice survival compared to littermate $Gata3^{fl/fl}$ (Figure 4E). Altogether, these results suggest that bladder ILC2s do not play a central role in bladder tumor development.

Discussion

In this study, we investigated the involvement of ILC2s in the bladder during tumor growth using mouse models. We found the mouse bladder as being particularly enriched in ILC2s at steady state, similar to the enrichment described in barrier tissues such as the lung. ILC subsets in the bladder are poorly described in the literature. Scharff et al. (43) are among the first to report bladder-resident ILC populations. Together with more recent studies (38, 44), they reported an increase of ILC3s in mouse bladders following uropathogenic *Escherichia coli* infection and highlighted their importance against the infection. Under steady-state conditions, they also suggested that ILC2s were the main ILC subset in mouse bladders, consistent with our own results (38, 44). Nevertheless, while the levels of ILC subsets differed between these studies, they consistently reported higher levels of bladder-infiltrating ILC3s at steady state compared to our results (38, 44). These differences could be potentially explained by differences in the lineage and/or gating strategies. The lack of specific markers for ILC subsets poses a challenge, as an overly permissive lineage would overestimate ILC subsets, whereas an overly restrictive lineage would underestimate them. Based on the differences observed in the literature regarding ILC3 subset, our lineage approach may be considered relatively restrictive. However, we were able to properly detect ILC3s in the lamina propria of the small intestines, which is a well-known homing sites for ILC3s, arguing that our lineage seems accurate and comprehensive. Further investigations are warranted to clarify this point.

In our study, we investigated the potential involvement of ILC2s in bladder tumor development using various approaches. Neutralizing ILC2 activation and function in mice through antibody blockade during bladder tumor growth suggested that ILC2 may not play a critical role in bladder tumor development. Nevertheless, it should be considered that all the factors involved in ILC2 pathways were not specifically targeted by the blocking antibodies used in our study, potentially leading to a partial neutralization of ILC2 activation and function. In addition to cytokine secretion and soluble factors, ILC2s can exert their functions through cell-to-cell contact (21), suggesting that direct interactions with other immune cells may contribute to the overall effects of ILC2s in the tumor microenvironment. To limit this bias in our investigations, we completed our study on ILC2s in bladder tumor development using transgenic ILC2-deficient mice. However, the absence of ILC2s in these mice did not affect the mice survival following bladder tumor challenge, in line with the results obtained when blocking IL-4/IL-13 or IL-5 signaling pathways, or IL-33/ST2 axis. Overall, these results suggest that ILC2 may not contribute significantly to bladder tumor development.

Although the involvement of ILC2s in mouse bladder tumor growth appeared marginal, our results have to be confirmed in bladder cancer patients. A recent study (45) reported ILC1s and ILC2s as the most frequent subsets infiltrating muscle invasive bladder tumors in patients, and low levels of ILC3s. Similarly to what we observed during mouse bladder tumor growth, higher levels of ILC1s were associated with more advanced tumor stages suggesting a potential role in disease progression. Notably, tumor-infiltrating ILC1s displayed an exhausted T_H17 -like phenotype suggesting potential functional impairment of ILC1s within the bladder. Additional studies are therefore required to elucidate the role of ILC1s in bladder tumor. Moreover, we previously reported higher levels of circulating ILC2s in MIBC patients at the time of the cystectomy compared to NMIBC patients or healthy donors (30). In the context of BCG therapy, our previous investigations in patients also suggested a potential role for ILC2s in bladder cancer recurrence, possibly through IL-13 secretion and MDSC recruitment (30). BCG therapy elicits a robust release of cytokines and chemokines within the bladder, which may potentially impact the role of ILC2s in the bladder tumor microenvironment as ILC2 plasticity and sensitivity to microenvironmental cues render their responses highly context-specific (46). In addition, ILC2s are known for their production of type 2 cytokines and their role in promoting T_H2 immune responses (47), thus they might be of important in the T_H1/T_H2 balance and in influencing treatment response during BCG therapy (48–51).

In summary, while ILC2s have been implicated in promoting tumor growth and immunosuppression in other cancer models, our study in bladder cancer suggests that ILC2-related pathways may not be the principal drivers of tumor development. However, further investigations of ILC infiltration in bladder tissues from spontaneous bladder tumor model and bladder cancer patients, with the assessment of effector cytokine secretion and activation or

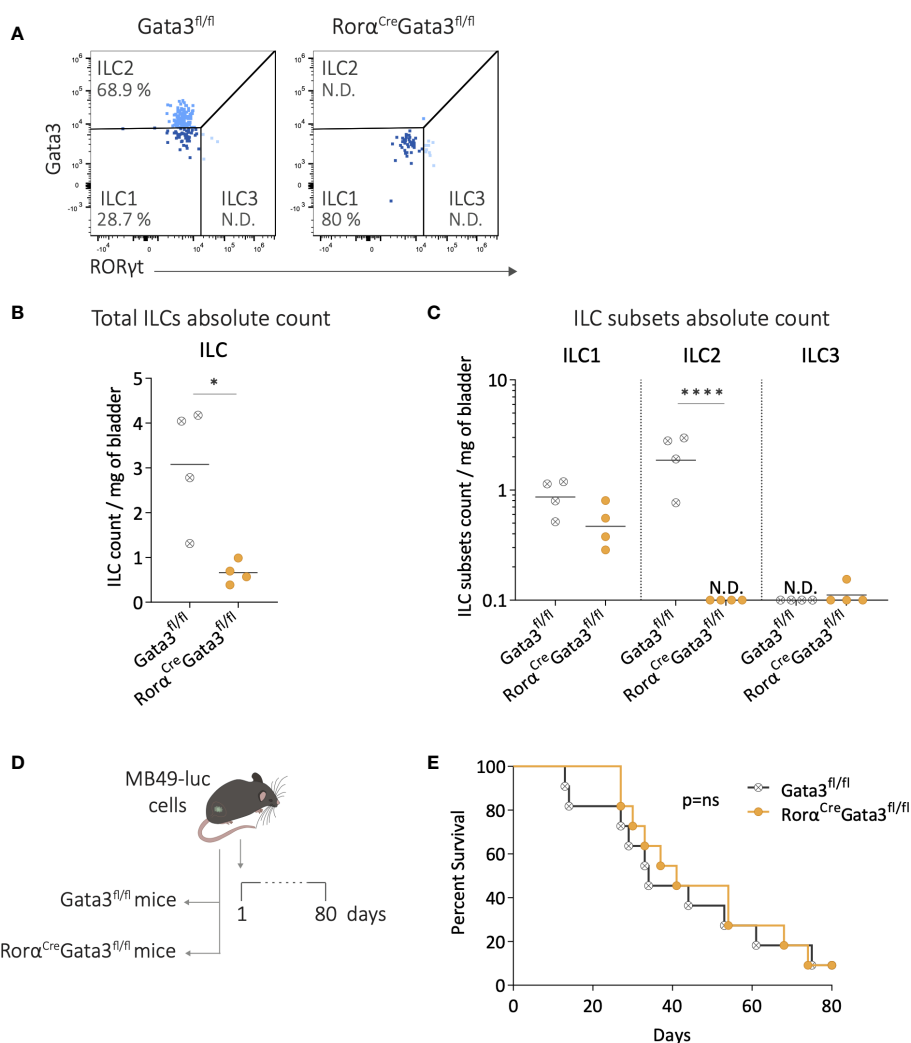


FIGURE 4

Depletion of ILC2s during bladder-tumor challenge. (A) Representative flow cytometry plots of ILC subsets from bladders of $Gata3^{fl/fl}$ and $Rora^{Cre}Gata3^{fl/fl}$ mice at steady state. Number per mg of bladder of (B) total ILCs, and (C) ILC subsets in $Gata3^{fl/fl}$ and $Rora^{Cre}Gata3^{fl/fl}$ mice at steady state. Horizontal lines represent the mean (B) or geometric mean (C), N.D. not detected. (D) Luciferase-expressing MB49 tumor cells (MB49-luc) were instilled in $Gata3^{fl/fl}$ and $Rora^{Cre}Gata3^{fl/fl}$ mice on day 1 followed by survival monitoring. (E) Survival curves of $Gata3^{fl/fl}$ (n=11) and $Rora^{Cre}Gata3^{fl/fl}$ (n=11) mice after MB49 bladder tumor instillation. Statistical significances were determined by parametric (B) t test or (C) one-way ANOVA followed by Bonferroni's test comparing the infiltration between $Gata3^{fl/fl}$ and $Rora^{Cre}Gata3^{fl/fl}$ mice. Log-rank test was performed as statistical analysis for survival curves. * $p \leq 0.05$; **** $p \leq 0.0001$; ns: not significant.

exhaustion markers, are warranted to clarify the involvement of ILC subsets in bladder cancer, including over the BCG treatment course.

glutamax-1 and sodium pyruvate complemented with 10 mM HEPES, 100U/mL of penicillin-streptomycin, and 10% FCS.

Materials and methods

Tumor cell line

MB49 cell line is derived from a carcinogen induced urothelial carcinoma in male C57Bl/6 mice (52). The cell line was provided by Prof. A. Loskog (Uppsala University, Sweden) and transfected with lentiviral vectors encoding for firefly luciferase (provided by Prof. D. Trono, EPFL, Switzerland) to generate luciferase (luc)-expressing MB49 cells (53). MB49-luc cells were cultured at 37°C in a humidified incubator with 5% CO₂, in DMEM containing

Mouse models

7 to 10-week-old female C57BL/6J OlaHsd mice were purchased from Envigo. Roratm1(cre)Ddmo mice (54) provided by Prof. P.G. Fallon (Trinity college, Ireland) were crossed with $Gata3^{fl/fl}$ mice (Taonic line 355) (55) ordered from the NIAID-Taonic repository, to generate $Rora^{Cre}Gata3^{fl/fl}$ mice (42). $Il33^{gfp/gfp}$ mice obtained through the RIKEN Center for Developmental Biology (Acc. No. CDB0631K) (56) were provided by Prof. S. Luther (University of Lausanne (UNIL), Switzerland). All mice were bred and housed at the animal facility of the University of Lausanne. All

in vivo experiments were conducted in accordance with the Swiss law and approval of the Cantonal Veterinary Office of Canton de Vaud, Switzerland.

MB49 orthotopic bladder tumor model

As previously described (57, 58), bladders of deeply anesthetized female mice were treated with 100 μ L of ethanol 22% for 15 min, followed by the intravesical instillation of 500 000 MB49-luc cells resuspended in 50 μ L of Hanks' Balanced Salt Solution (HBSS) using catheters. To monitor tumor growth, mice were administered an intraperitoneal injection of D-luciferin (150 μ g/g of body weight; Biosynth) 15 min before measuring bioluminescence of MB49-luc tumor cells with a Xenogen imaging system (Xenogen/IVIS lumina III). In order to avoid bias in the comparison of tumor growth data, bioluminescence imaging was not performed as soon as one mouse died in either of the tested groups. In addition, after the first 3 weeks of tumor growth, bioluminescence is often lost, due to presence of necrotic tumors and/or low tumor-perfusion, preventing tumor-penetration of the injected luciferin (53, 59), thereby tumor growth was monitored by palpation, hematuria, and overall health status of the mice.

Preparation of mouse organ cell suspensions

Mice were sacrificed by CO₂ inhalation and organs were harvested. Single-cell suspensions from spleen were obtained through mechanical dissociation by scratching the spleen onto a 70- μ m filter, followed by a red blood cell lysis buffer treatment, and subsequently filtered through a 40- μ m filter. Single-cell suspensions from lymph nodes were obtained through mechanical dissociation by scratching the lymph nodes onto a 40- μ m filter. Bladder and lungs were minced and digested in 2 mL/organ of digestion buffer containing 1 mg/mL collagenase/dispase or collagenase D, 0.1 mg/mL DNase I, and FCS 5% in Iscove's modified Dulbecco's medium with glutamax-1, for 45 min at 37°C in a rotating shaker. After stopping the digestion with FACS buffer (PBS, 2 mM EDTA, and 0.2% BSA), bladder cell suspensions were scratched onto a 40- μ m filter, while lung cell suspensions were scratched onto a 70- μ m filter and subsequently filtered through a 40- μ m filter. Cell suspensions were centrifuged for 10 min at 1000 rpm at room temperature and lung pelleted cells were then treated with red blood cells lysis buffer. All cell suspensions from spleen, lymph nodes, bladder and lung were resuspended in DMEM containing glutamax-1 and sodium pyruvate complemented with 10 mM HEPES, 100 U/mL of penicillin-streptomycin, and 10% FCS. Mice without tumors and tumor-bearing mice at day 5 were pooled by 2 to 3 before processing the organs to increase the number of cells recovered from bladder and ILN.

For the small intestines, fat and Peyer's patches were removed from the intestine walls, and intestinal contents were removed by flushing with cold PBS. Small intestines were opened longitudinally

to remove the mucus then cut in 1-cm pieces. The pieces were shaken several times in PBS to remove any residual intestine contents. Subsequently, intestinal pieces were incubated in 20 mL of intestine epithelial fraction buffer containing HBSS, EDTA 5mM, dithiothreitol 1 mM, and FCS 5% for 20 min at 37°C in a shaker at 250 rpm. After 20 min the supernatant with the epithelial fraction was discarded and the fragments rinsed with PBS. This step was repeated twice. The intestinal fragments were then collected and digested a first time in 10 mL of digestion buffer with RPMI medium, Collagenase/dispase 1 mg/mL, DNase 20 μ g/mL, and FCS 10% for 45 min at 37°C in a shaker at 250 rpm. After 45 min, the supernatant was collected through a 70- μ m filter and resuspended with PBS-FCS 2%, and the intestinal fragments were digested a second time for 30 min at 37°C in a shaker at 250 rpm. After 30 min, the supernatants were collected through a 70- μ m filter, centrifuged for 15 min at 400 x g and resuspended with PBS-FCS 2%.

Flow cytometry analysis

Recovered cells from mouse samples were stained and analyzed by flow cytometry. The following antibodies were used for staining in mouse samples: anti-GATA3 (BD Biosciences, Cat# 563349, BV421, clone L50-823), anti-ROR γ t (Thermo Fisher Scientific, Cat# 61-6981-80, PE/eF610, clone B2D), anti-CD90.2 (Thermo Fisher Scientific, Cat# 47-0902-82, APCeF780, clone 53-2.1), anti-CD127 (Biolegend, Cat# 135012, APC, clone A7R34), anti-CD45 (Biolegend, Cat# 103128, AF700, and BD Biosciences, Cat# 564279, BUV395, clone 30-F11), anti-CD3 (Thermo Fisher Scientific, Cat# 11-0031-85, FITC, and BD Biosciences, Cat# 745836, BB700, clone 145-2C11), anti-CD19 (Thermo Fisher Scientific, Cat# 11-0193-82, FITC, clone 1D3), anti-FCeRI (Biolegend, Cat# 134306, FITC, clone MAR-1), anti-CD5 (Biolegend, Cat# 100605, FITC, clone 53-7.3), anti-TER119 (Biolegend, Cat# 116206, FITC, clone TER-119), anti-GR-1 (Biolegend, Cat# 108405, FITC, clone RB6-8C5), anti-CD11c (Biolegend, Cat# 117306, FITC, clone N418), anti-F4/80 (Biolegend, Cat# 123108, FITC, clone BM8), anti-CD49b (Thermo Fisher Scientific, Cat# 11-5971-85, FITC, and BD Biosciences, Cat# 562453, PE-CF594, clone DX5), anti-CD11b (Biolegend, Cat# 101206, FITC, and BD Biosciences, Cat# 612977, BUV661, clone M1/70), anti-TCR γ δ (Thermo Fisher Scientific, Cat# 11-5711-85, FITC, clone GL-3), anti-TCR β (Biolegend, Cat# 109206, FITC, clone H57-597), anti-CD8 (Biolegend, Cat# 100706, FITC, and BD Biosciences, Cat# 563152, BV605, clone 53-6.7), anti-B220 (Thermo Fisher Scientific, Cat# 11-0452-85, FITC, clone RA3-6B2), anti-CD4 (BD Biosciences, Cat# 612761, BUV737, clone GK1.5), anti-ST2 (Thermo Fisher Scientific, Cat# 25-9335-82, PE/Cy7, clone RMST2-2). For cell surface antigen staining, cells were incubated for 30 minutes at 4°C using antibodies described above, and an amine reactive dye (LIVE/DEADTM Fixable Aqua Dead Cell Stain Kit, Thermo Fisher Scientific) was used for dead cell exclusion according to the manufacturer's instructions. To block unspecific binding of antibodies, mouse serum was used. After extracellular staining, cells were fixed and permeabilized, and intracellular

staining was performed according to manufacturer instruction, using the Foxp3/Transcription Factor Staining Buffer Set (Thermo Fisher Scientific). Sample acquisition was performed on Cytoflex LX1 (Beckman Coulter) or LSRFortessa (Becton Dickinson), and data were analyzed using FlowJo software.

In vitro stimulation for IL-13 secretion

Recovered cell suspension from bladder of naïve or bladder tumor-bearing mice were seeded in 24-well plates (between 10^6 and 2.10^6 cells per well) and stimulated for 4 h at 37°C with phorbol 12-myristate 13-acetate (PMA) and ionomycin (Cell stimulation cocktail 500X, Thermo Fisher Scientific, Cat# 00-4970-03) or left unstimulated (culture medium only). After 2h of stimulation, brefeldin A and monensin were added in all the wells (Protein Transport Inhibitor Cocktail 500X, Thermo Fisher Scientific, Cat# 00-4980-93) for intracellular retention of the induced cytokine expression. Following stimulation, cells were collected for intracellular staining of ILC panel and IL-13 (Thermo Fisher Scientific, Cat# 46-7133-82, PerCP-eF710, clone eBio13A).

Cytokines array in mouse bladder during tumor growth

Bladders from tumor-free mice (naïve) and during tumor growth (day 5, 10, and 13) were homogenized in PBS with a cocktail of protease inhibitors containing aprotinin (10 µg/mL, Sigma-Aldrich), leupeptin (10 µg/mL, Tocris), and pepstatin (10 µg/mL, Tocris) using a tissue grinder. Bladders without tumors and 5 days after tumor implantation were pooled by 2 before processing. After homogenization, Triton™ X-100 (Sigma-Aldrich) was added to a final concentration of 1%. Samples were frozen on dry ice, thawed and centrifuge at 10,000 x g for 5 minutes at 4°C to remove cellular debris. Samples were stored at -80°C until further analysis. Sample total protein concentrations were quantified using a Pierce BCA Protein Assay Kit (Thermo Fisher Scientific) following the manufacturer protocol for 96-well plate procedure. Finally, a Luminex assay was done according to the manufacturer instructions (Bio-Plex Pro Mouse Cytokine assays from Bio-Rad) for quantification of the following cytokines: IL-4, IL-5, IL-13, IL-25, IL-33. Samples were analyzed with a Bio-Plex 200 system.

Blocking antibody treatments in mice

To neutralize IL-4R α , mice were injected intraperitoneally with blocking antibodies α -CD124 (100 µg/injection/mouse; BD Biosciences, Cat# 552288, clone mIL4R-M1) or rat IgG2a k isotype control (BioXcell, Cat# BE0089, clone 2A3) diluted in PBS at day 1-3-5-8-11 since bladder-tumor implantation. To neutralize IL-5, mice were injected intraperitoneally with blocking antibodies α -IL-5 (300 µg/injection/mouse; BioXcell, Cat# BE0198, clone

TRFK5) or rat IgG1a k isotype control (BioXcell, Cat# BE0088, clone HRPN) diluted in PBS at day -2-2-6-10-15-19-24-29-34 and bladder-tumor implantation at day 1. To neutralize IL-33R α , mice were injected intraperitoneally with blocking antibodies α -ST2 (100 µg/injection/mouse; Biolegend, Cat# 146604, clone DIH4), or rat IgG1 k isotype control (Biolegend, Cat# 400457, clone RTK2071) diluted in PBS at day 1-3-5-8-11 since bladder-tumor implantation.

Quantification and statistical analysis

Statistical analyses were performed using the GraphPad Prism 9 software as indicated in the figure legends. Recurrence-free and progression-free survival rates were evaluated using Kaplan-Meier estimator.

Data availability statement

The original contributions presented in the study are included in the article/[Supplementary Material](#). Further inquiries can be directed to the corresponding author.

Ethics statement

The animal study was approved by Swiss Federal Veterinary Office (SFVO). The study was conducted in accordance with the local legislation and institutional requirements.

Author contributions

AS: Data curation, Formal Analysis, Investigation, Methodology, Writing – original draft. SD-P: Writing – review & editing, Investigation, Methodology. VC: Writing – review & editing, Investigation, Methodology. LP: Investigation, Writing – review & editing. PF: Writing – review & editing, Resources. JZ: Resources, Writing – review & editing. BR: Resources, Validation, Writing – review & editing, Methodology. DN-H: Funding acquisition, Resources, Writing – review & editing, Methodology. LD: Conceptualization, Funding acquisition, Project administration, Resources, Supervision, Validation, Writing – original draft, Writing – review & editing.

Funding

The author(s) declare financial support was received for the research, authorship, and/or publication of this article. This work was funded by grants from the Swiss Cancer Research foundation (KFS-4101-02-2017 and KFS-5105-08-2020-R) and a Ferring Innovation Grant.

Acknowledgments

Authors acknowledge Prof. Sanjiv Luther (UNIL, Switzerland) for providing the Il33^{gfp/gfp} mice.

Conflict of interest

The authors declare that the research was conducted in the absence of any commercial or financial relationships that could be construed as a potential conflict of interest.

The author(s) declared that they were an editorial board member of Frontiers, at the time of submission. This had no impact on the peer review process and the final decision.

References

- Teoh JYC, Huang J, Ko WYK, Lok V, Choi P, Ng CF, et al. Global trends of bladder cancer incidence and mortality, and their associations with tobacco use and gross domestic product per capita. *Eur Urology*. (2020) 78(6):893–906. doi: 10.1016/j.eururo.2020.09.006
- Sanli O, Dobruch J, Knowles MA, Burger M, Alemozaffar M, Nielsen ME, et al. Bladder cancer. *Nat Rev Dis Primers*. (2017) 3(1):17022. doi: 10.1038/nrdp.2017.22
- Freedman ND. Association between smoking and risk of bladder cancer among men and women. *JAMA* (2011) 306(7):737. doi: 10.1001/jama.2011.1142
- Witjes JA, Bruins HM, Cathomas R, Compérat EM, Cowan NC, Gakis G, et al. European association of urology guidelines on muscle-invasive and metastatic bladder cancer: summary of the 2020 guidelines. *Eur Urology*. (2021) 79(1):82–104. doi: 10.1016/j.eururo.2020.03.055
- Babjuk M, Burger M, Capoun O, Cohen D, Compérat EM, Dominguez Escrig JL, et al. European association of urology guidelines on non-muscle-invasive bladder cancer (Ta, T1, and carcinoma in situ). *Eur Urology*. (2022) 81(1):75–94. doi: 10.1016/j.eururo.2021.08.010
- Lobo N, Brooks NA, Zlotta AR, Cirillo JD, Boorjian S, Black PC, et al. 100 years of Bacillus Calmette–Guérin immunotherapy: from cattle to COVID-19. *Nat Rev Urol*. (2021) 18(10):611–22. doi: 10.1038/s41585-021-00481-1
- Vivier E, Artis D, Colonna M, Diefenbach A, Di Santo JP, Eberl G, et al. Innate lymphoid cells: 10 years on. *Cell* (2018) 174(5):1054–66. doi: 10.1016/j.cell.2018.07.017
- Colonna M. Innate lymphoid cells: diversity, plasticity, and unique functions in immunity. *Immunity* (2018) 48(6):1104–17. doi: 10.1016/j.immuni.2018.05.013
- Simoni Y, Newell EW. Dissecting human ILC heterogeneity: more than just three subsets. *Immunology* (2018) 153(3):297–303. doi: 10.1111/imm.12862
- Hoyle T, Klose CSN, Souabni A, Turqueti-Neves A, Pfeifer D, Rawlins EL, et al. The transcription factor GATA-3 controls cell fate and maintenance of type 2 innate lymphoid cells. *Immunity* (2012) 37(4):634–48. doi: 10.1016/j.immuni.2012.06.020
- Wong SH, Walker JA, Jolin HE, Drynan LF, Hams E, Camelo A, et al. Transcription factor ROR α is critical for nuocyte development. *Nat Immunol* (2012) 13(3):229–36. doi: 10.1038/ni.2208
- Ferreira ACF, Szeto ACH, Heycock MWD, Clark PA, Walker JA, Crisp A, et al. ROR α is a critical checkpoint for T cell and ILC2 commitment in the embryonic thymus. *Nat Immunol* (2021) 22(2):166–78. doi: 10.1038/s41590-020-00833-w
- Kim CH, Hashimoto-Hill S, Kim M. Migration and tissue tropism of innate lymphoid cells. *Trends Immunol* (2016) 37(1):68–79. doi: 10.1016/j.it.2015.11.003
- Klose CSN, Artis D. Innate lymphoid cells as regulators of immunity, inflammation and tissue homeostasis. *Nat Immunol* (2016) 17(7):765–74. doi: 10.1038/ni.3489
- Schulz-Kuhnt A, Wirtz S, Neurath MF, Atraya I. Regulation of human innate lymphoid cells in the context of mucosal inflammation. *Front Immunol* (2020) 11:1062. doi: 10.3389/fimmu.2020.01062
- Panda SK, Colonna M. Innate lymphoid cells in mucosal immunity. *Front Immunol* (2019) 10:861. doi: 10.3389/fimmu.2019.00861
- Duan Z, Liu M, Yuan L, Du X, Wu M, Yang Y, et al. Innate lymphoid cells are double-edged swords under the mucosal barrier. *J Cell Mol Med* (2021) 25(18):8579–87. doi: 10.1111/jcmm.16856

Publisher's note

All claims expressed in this article are solely those of the authors and do not necessarily represent those of their affiliated organizations, or those of the publisher, the editors and the reviewers. Any product that may be evaluated in this article, or claim that may be made by its manufacturer, is not guaranteed or endorsed by the publisher.

Supplementary material

The Supplementary Material for this article can be found online at: <https://www.frontiersin.org/articles/10.3389/fimmu.2023.1335326/full#supplementary-material>

- Chiossone L, Dumas PY, Vienne M, Vivier E. Natural killer cells and other innate lymphoid cells in cancer. *Nat Rev Immunol* (2018) 18(11):671–88. doi: 10.1038/s41577-018-0061-z
- Jacquelot N, Seillet C, Vivier E, Belz GT. Innate lymphoid cells and cancer. *Nat Immunol* (2022) 23(3):371–9. doi: 10.1038/s41590-022-01127-z
- Ruf B, Greten TF, Korangy F. Innate lymphoid cells and innate-like T cells in cancer — at the crossroads of innate and adaptive immunity. *Nat Rev Cancer*. (2023) 23(6):351–71. doi: 10.1038/s41568-023-00562-w
- Wu L, Zhao W, Tang S, Chen R, Ji M, Yang X. Role of ILC2s in solid tumors: facilitate or inhibit? *Front Immunol* (2022) 13:886045. doi: 10.3389/fimmu.2022.886045
- Okuyama Y, Okajima A, Sakamoto N, Hashimoto A, Tanabe R, Kawajiri A, et al. IL-33-ILC2 axis promotes anti-tumor CD8⁺ T cell responses via OX40 signaling. *Biochem Biophys Res Commun* (2022) 637:9–16. doi: 10.1016/j.bbrc.2022.11.006
- Jacquelot N, Seillet C, Wang M, Pizzolla A, Liao Y, Hediyyeh-zadeh S, et al. Blockade of the co-inhibitory molecule PD-1 unleashes ILC2-dependent antitumor immunity in melanoma. *Nat Immunol* (2021) 22(7):851–64. doi: 10.1038/s41590-021-00943-z
- Moral JA, Leung J, Rojas LA, Ruan J, Zhao J, Sethna Z, et al. ILC2s amplify PD-1 blockade by activating tissue-specific cancer immunity. *Nature* (2020) 579(7797):130–5. doi: 10.1038/s41586-020-2015-4
- Yuan X, Rasul F, Nashan B, Sun C. Innate lymphoid cells and cancer: Role in tumor progression and inhibition. *Eur J Immunol* (2021) 51(9):2188–205. doi: 10.1002/eji.202049033
- Schuijs MJ, Png S, Richard AC, Tsyben A, Hamm G, Stockis J, et al. ILC2-driven innate immune checkpoint mechanism antagonizes NK cell antimetastatic function in the lung. *Nat Immunol* (2020) 21(9):998–1009. doi: 10.1038/s41590-020-0745-y
- Xu X, Ye L, Zhang Q, Shen H, Li S, Zhang X, et al. Group-2 innate lymphoid cells promote HCC progression through CXCL2-neutrophil-induced immunosuppression. *Hepatology* (2021) 74(5):2526–43. doi: 10.1002/hep.31855
- Jovanovic IP, Pejnovic NN, Radosavljevic GD, Pantic JM, Milovanovic MZ, Arsenijevic NN, et al. Interleukin-33/ST2 axis promotes breast cancer growth and metastases by facilitating intratumoral accumulation of immunosuppressive and innate lymphoid cells: IL-33 enhances breast cancer progression. *Int J Cancer*. (2014) 134(7):1669–82. doi: 10.1002/ijc.28481
- Jou E, Rodriguez-Rodriguez N, Ferreira ACF, Jolin HE, Clark PA, Sawmynaden K, et al. An innate IL-25–ILC2–MDSC axis creates a cancer-permissive microenvironment for *Apc* mutation-driven intestinal tumorigenesis. *Sci Immunol* (2022) 7(72):eabn0175. doi: 10.1126/sciimmunol.abn0175
- Chevalier MF, Trabanelli S, Racle J, Salomé B, Cesson V, Gharbi D, et al. ILC2-modulated T cell-to-MDSC balance is associated with bladder cancer recurrence. *J Clin Invest* (2017) 127(8):2916–29. doi: 10.1172/JCI89717
- Junttila IS. Tuning the cytokine responses: an update on interleukin (IL)-4 and IL-13 receptor complexes. *Front Immunol* (2018) 9:888. doi: 10.3389/fimmu.2018.00888
- Andrews AL, Holloway JW, Holgate ST, Davies DE. IL-4 receptor alpha is an important modulator of IL-4 and IL-13 receptor binding: implications for the development of therapeutic targets. *J Immunol* (2006) 176(12):7456–61. doi: 10.4049/jimmunol.176.12.7456

33. Kasaian MT, Marquette K, Fish S, DeClercq C, Agostinelli R, Cook TA, et al. An IL-4/IL-13 dual antagonist reduces lung inflammation, airway hyperresponsiveness, and IgE production in mice. *Am J Respir Cell Mol Biol* (2013) 49(1):37–46. doi: 10.1165/rcmb.2012-0500OC
34. Arnold IC, Artola-Borán M, Tallón de Lara P, Kyburz A, Taube C, Ottemann K, et al. Eosinophils suppress Th1 responses and restrict bacterially induced gastrointestinal inflammation. *J Exp Med* (2018) 215(8):2055–72. doi: 10.1084/jem.20172049
35. Frisbee AL, Saleh MM, Young MK, Leslie JL, Simpson ME, Abhyankar MM, et al. IL-33 drives group 2 innate lymphoid cell-mediated protection during *Clostridium difficile* infection. *Nat Commun* (2019) 10(1):2712. doi: 10.1038/s41467-019-10733-9
36. Topczewska PM, Rompe ZA, Jakob MO, Stamm A, Leclère PS, Preußer A, et al. ILC2 require cell-intrinsic ST2 signals to promote type 2 immune responses. *Front Immunol* (2023) 14:1130933. doi: 10.3389/fimmu.2023.1130933
37. Wu Y, Shi W, Wang H, Yue J, Mao Y, Zhou W, et al. Anti-ST2 nanoparticle alleviates lung inflammation by targeting ILC2s-CD4+T response. *Int J Nanomedicine*. (2020) 15:9745–58. doi: 10.2147/IJN.S268282
38. Huang J, Fu L, Huang J, Zhao J, Zhang X, Wang W, et al. Group 3 innate lymphoid cells protect the host from the uropathogenic *Escherichia coli* infection in the bladder. *Advanced Science*. (2022) 9(6):2103303. doi: 10.1002/advs.202103303
39. Qiu X, Qi C, Li X, Fang D, Fang M. IL-33 deficiency protects mice from DSS-induced experimental colitis by suppressing ILC2 and Th17 cell responses. *Inflammation Res* (2020) 69(11):1111–22. doi: 10.1007/s00011-020-01384-4
40. Flamar AL, Klose CSN, Moeller JB, Mahlaköiv T, Bessman NJ, Zhang W, et al. Interleukin-33 induces the enzyme tryptophan hydroxylase 1 to promote inflammatory group 2 innate lymphoid cell-mediated immunity. *Immunity* (2020) 52(4):606–619.e6. doi: 10.1016/j.immuni.2020.02.009
41. Cayrol C, Girard JP. IL-33: an alarmin cytokine with crucial roles in innate immunity, inflammation and allergy. *Curr Opin Immunol* (2014) 31:31–7. doi: 10.1016/j.coi.2014.09.004
42. Omata Y, Frech M, Primbs T, Lucas S, Andreev D, Scholtysek C, et al. Group 2 innate lymphoid cells attenuate inflammatory arthritis and protect from bone destruction in mice. *Cell Rep* (2018) 24(1):169–80. doi: 10.1016/j.celrep.2018.06.005
43. Scharff AZ, Rousseau M, Mariano LL, Canton T, Consiglio CR, Albert ML, et al. Sex differences in IL-17 contribute to chronicity in male versus female urinary tract infection. *JCI Insight* (2019) 4(13):e122998. doi: 10.1172/jci.insight.122998
44. Riding AM, Loudon KW, Guo A, Ferdinand JR, Lok LSC, Richoz N, et al. Group 3 innate lymphocytes make a distinct contribution to type 17 immunity in bladder defence. *iScience* (2022) 25(7):104660. doi: 10.1016/j.isci.2022.104660
45. Mukherjee N, Ji N, Tan X, Lin C, Rios E, Chen C, et al. Bladder tumor ILC1s undergo Th17-like differentiation in human bladder cancer. *Cancer Med* (2021) 10(20):7101–10. doi: 10.1002/cam4.4243
46. Bal SM, Golebski K, Spits H. Plasticity of innate lymphoid cell subsets. *Nat Rev Immunol* (2020) 20(9):552–65. doi: 10.1038/s41577-020-0282-9
47. Mirchandani AS, Besnard AG, Yip E, Scott C, Bain CC, Cerovic V, et al. Type 2 innate lymphoid cells drive CD4+ Th2 cell responses. *J Immunol* (2014) 192(5):2442–8. doi: 10.4049/jimmunol.1300974
48. Saint F, Patard JJ, Maille P, Soyeux P, Hoznek A, Salomon L, et al. Prognostic value of a T helper 1 urinary cytokine response after intravesical bacillus Calmette-Guérin treatment for superficial bladder cancer. *J Urol*. (2002) 167(1):364–7. doi: 10.1016/S0022-5347(05)65469-9
49. Watanabe E, Matsuyama H, Matsuda K, Ohmi C, Tei Y, Yoshihiro S, et al. Urinary interleukin-2 may predict clinical outcome of intravesical bacillus Calmette-Guérin immunotherapy for carcinoma in situ of the bladder. *Cancer Immunol Immunother*. (2003) 52(8):481–6. doi: 10.1007/s00262-003-0384-9
50. Pichler R, Gruenbacher G, Culig Z, Brunner A, Fuchs D, Fritz J, et al. Intratumoral Th2 predisposition combines with an increased Th1 functional phenotype in clinical response to intravesical BCG in bladder cancer. *Cancer Immunol Immunother*. (2017) 66(4):427–40. doi: 10.1007/s00262-016-1945-z
51. Saint F, Kurth N, Maille P, Vordos D, Hoznek A, Soyeux P, et al. Urinary IL-2 assay for monitoring intravesical bacillus Calmette-Guérin response of superficial bladder cancer during induction course and maintenance therapy: Urinary IL-2 Assay for Monitoring Intravesical BCG. *Int J Cancer*. (2003) 107(3):434–40. doi: 10.1002/ijc.11352
52. Summerhayes IC, Franks LM. Effects of donor age on neoplastic transformation of adult mouse bladder epithelium in vitro. *J Natl Cancer Inst* (1979) 62(4):1017–23. doi: 10.1093/jnci/62.4.1017
53. Domingos-Pereira S, Cesson V, Chevalier MF, Derré L, Jichlinski P, Nardelli-Haeffliger D. Preclinical efficacy and safety of the Ty21a vaccine strain for intravesical immunotherapy of non-muscle-invasive bladder cancer. *Oncoimmunology* (2017) 6(1):e1265720. doi: 10.1080/2162402X.2016.1265720
54. Wu CS, Zhu J, Wager-Miller J, Wang S, O'Leary D, Monory K, et al. Requirement of cannabinoid CB(1) receptors in cortical pyramidal neurons for appropriate development of corticothalamic and thalamocortical projections. *Eur J Neurosci* (2010) 32(5):693–706. doi: 10.1111/j.1460-9568.2010.07337.x
55. Zhu J, Min B, Hu-Li J, Watson CJ, Grinberg A, Wang Q, et al. Conditional deletion of Gata3 shows its essential function in T(H)1-T(H)2 responses. *Nat Immunol* (2004) 5(11):1157–65. doi: 10.1038/nii1128
56. Oboki K, Ohno T, Kajiwaru N, Arae K, Morita H, Ishii A, et al. IL-33 is a crucial amplifier of innate rather than acquired immunity. *Proc Natl Acad Sci U S A*. (2010) 107(43):18581–6. doi: 10.1073/pnas.1003059107
57. Domingos-Pereira S, Sathiyandan K, La Rosa S, Polák L, Chevalier MF, Martel P, et al. Intravesical ty21a vaccine promotes dendritic cells and T cell-mediated tumor regression in the MB49 bladder cancer model. *Cancer Immunol Res* (2019) 7(4):621–9. doi: 10.1158/2326-6066.CIR-18-0671
58. Günther JH, Jurczok A, Wulf T, Brandau S, Deinert I, Jocham D, et al. Optimizing syngeneic orthotopic murine bladder cancer (MB49). *Cancer Res* (1999) 59(12):2834–7.
59. Jurczok A, Fornara P, Söling A. Bioluminescence imaging to monitor bladder cancer cell adhesion in vivo: a new approach to optimize a syngeneic, orthotopic, murine bladder cancer model. *BJU Int* (2008) 101(1):120–4. doi: 10.1111/j.1464-410X.2007.07193.x